

Investigation of solid lipid nanoparticles as oral delivery of Paclitaxel for enhanced absorption

Jagruati DESAI^{1*}, Swayamprakash PATEL¹, Arehalli MANJAPPA², Alkesh PATEL³, Twinkle PATEL¹

¹ Department of Pharmaceutics and Pharmaceutical Technology, Ramanbhai Patel College of Pharmacy, Charotar University of Science and technology (CHARUSAT), CHARUSAT Campus, Changa-388 421, India.

² Department of Pharmaceutics, Vasantidevi Patil Institute of Pharmacy, Kodoli, Taluka Panhala, District Kolhapur, Maharashtra, India.

³ Department of Pharmacology, Ramanbhai Patel College of Pharmacy, Charotar University of Science and technology (CHARUSAT), CHARUSAT Campus, Changa-388 421, India.

* Corresponding Author. E-mail: jagrutidesai.ph@charusat.ac.in (J.D.); Tel. 02697-265147.

Received: 03 March 2023 / Revised: 07 September 2023 / Accepted: 07 September 2023

ABSTRACT: Paclitaxel is an anticancer drug that has poor oral bioavailability (>10%) because of its poor solubility in aqueous medium, poor permeability, and is a substrate of poly-glycoprotein and CYP450 metabolism. The current study intends to create Paclitaxel-loaded solid lipid nanoparticles (SLNs) to overcome these limitations. The nanoparticles were formulated through an emulsification-solvent evaporation method and freeze-dried. To optimize the nanoparticle formulation, the box-behnken design was adopted. The final formulation had a particle size of 190 nm with 88.79% drug entrapment. The *in-vitro* release study for 24 hr showed a 1.6-fold increase in drug release in the dissolution of paclitaxel from SLNs in comparison to drug suspension. A 2.4-fold increase in bioavailability of the drug *in-vivo* was obtained compared to the commercial formulation. Thus, a promising carrier for PTX was developed that could increase its efficiency and alleviate the dose-dependent side effects.

KEYWORDS: Paclitaxel; Intestinal permeability; solubility; M-cell uptake.

1. INTRODUCTION

The peroral route has traditionally been the preferred method of medication administration among the several available routes due to various factors, such as good patient compliance, ease of administration and cost-effectiveness [1]. This route involves taxols with a wide surface area offering the opportunity for drug adhesion and absorption, making it more preferable than other routes [2]. However, drug absorption through this route is more complicated compared to other pathways. Oral drugs are mostly absorbed in the stomach, necessitating that drugs dissolve in gastric fluid. Delivering hydrophobic molecules with unstable metabolism is a challenging aspect of systemic oral delivery [3]. Numerous new chemical entities with potential therapeutic action have been developed. However, most drugs have low solubility and/or permeability, leading to decreased bioavailability when delivered orally [4]. To address the limitations of the oral route, nanoparticles formulations are being explored. These formulations entrap and protect the active ingredient, releasing it in a controlled and sustained manner. This not only improves the solubilization of the drug in gastro-intestinal tract (GIT) but also addresses other factors that contribute to its low solubility. Many hydrophobic drug molecules [5,6] have already been incorporated into a solid lipid matrix to increase their bioavailability. This approach offers advantages such as enhanced bioavailability, minimized side effects, reduced drug concentration fluctuation and low required doses [7].

Paclitaxel (PTX) is a natural substance derived from the Taxol product, used to treat various types of cancer, making it an important drug in chemotherapy. PTX is effective against a wide range of tumors [8]. However, it falls under the BCS class IV category due to its poorly aqueous solubility and permeability [9,10] necessitating the addition of several solvents and co-solvent during its preparation for improved solubilization. The initial marketed formulation of PTX, Taxol[®] comprised a 1:1 combination of cremophor EL (crEL) and ethanol, used as an infusion formulation. Unfortunately crEL, diluting vehicle, leads to severe

How to cite this article: Desai J, Patel S, Manjappa A, Patel A, Patel T. Investigation of solid lipid nanoparticles as oral delivery of Paclitaxel for enhanced absorption. J Res Pharm. 2024; 28(3): 781-796.

side effect such as hypersensitivity (like nephrotoxicity, cardiotoxicity, neurotoxicity and neutropenia) and peripheral neuropathy. Additionally, crEL contributes to non-linear pharmacokinetic profile and complicates co-administration with other anti-tumor drugs [11]. Taxol® also suffered from short physical stability, short half-lives, large distribution volumes and rapid elimination from the body, resulting in partial accumulation in cancer cells with comparatively high drug exposure to non-cancer cells. This non-specific bio-distribution of PTX leads to increased toxicity and reduced therapeutic indices of the drug [12]. To overcome limitations associated with the oral route, such as solubility issues, fast metabolism and excessive drug plasma fluctuations, recent advancements have been made in the application of lipidic drug delivery systems for peroral administration of hydrophobic molecules. These lipidic systems have been shown to enhance the bioavailability of hydrophobic molecules by maintaining the active moiety in the dissolved form within the lipid phase until absorption, overcoming barriers of poor dissolution [13]. The diverse melting points of lipids offer an advantage in incorporating various drugs with potential degradation issues at their melting points.

Different lipid based formulations, such as liposomes [14,15] microemulsion [16], nanoparticles [3,8,17], and micelles [18] have been investigated to improve the solubility and enhance the permeability of hydrophobic molecules. Among these, lipid-based systems like solid lipid nanoparticles have emerged as efficient carriers in oral drug delivery. SLNs are aqueous colloidal dispersions with a matrix comprising biodegradable lipids, ranging in size from 50 to 500 nm. These nanocarriers, combined with lipidic properties, provide a solid structure at atmospheric temperature, stabilized by suitable surfactants, primarily ionic surfactants [19]. The solid matrix of SLNs effectively protects the integrated medicine from chemical deterioration in an *in-vivo* environment and offers flexibility in controlling drug release profiles. The lipid moiety in SLNs enhances the solubility of poorly soluble drugs, thereby increasing their bioavailability making SLNs efficient for oral delivery of lipophilic drugs. SLN combine the advantages of various colloidal carriers in their class, such as physical stability, protection of labile drugs from degradation, and good tolerability [20]. They are also reported to increase the bioavailability of drugs that undergo first-pass metabolism by direct uptake through M-cells, followed by entry into the lymphatic system [6]. These nanocarriers can be effectively directed via various routes, including peroral, ophthalmic, parenteral, transdermal and rectal routes [21,22]. Additionally, SLNs offer unique advantage of avoiding the use of organic solvents and the requirement for heavy instrument over other formulating approaches, enabling fast and efficient large-scale production [18]. The lipid matrix of the SLNs consists of physiologically compatible lipids that enable the emulsifiable and encapsulation of PTX, leading to an increase in its solubility. Furthermore, intact nanoparticles could enhance lymphatic absorption and reduce the risk of PTX toxicity [23,24]. Hence, in this work, we formulated solid lipid nanoparticles of PTX, optimized the formulation and characterized them.

2. RESULTS AND DISCUSSION

2.1. Selection of lipid

In Figure 1, the results of the experiment revealed the amount of PTX required to dissolve in different melted lipids. Among all the lipids tested, Imwitor 900K exhibited the lowest quantity needed to dissolve 5 mg of the drug, indicating a higher solubility of the drug in this lipid compared to the other solid lipids tested. Based on this finding, Imwitor 900K was selected as the suitable solid lipid for further formulation development. The higher drug solubility in Imwitor 900K makes it a favorable choice for the development of PTX-loaded solid lipid nanoparticles (SLNs). Utilizing Imwitor 900K as the lipid matrix can potentially enhance the drug's bioavailability and improve its therapeutic efficacy. This selection is a crucial step in the formulation development process, as it determines the carrier's ability to efficiently encapsulate and deliver the drug while ensuring its stability during storage and administration.

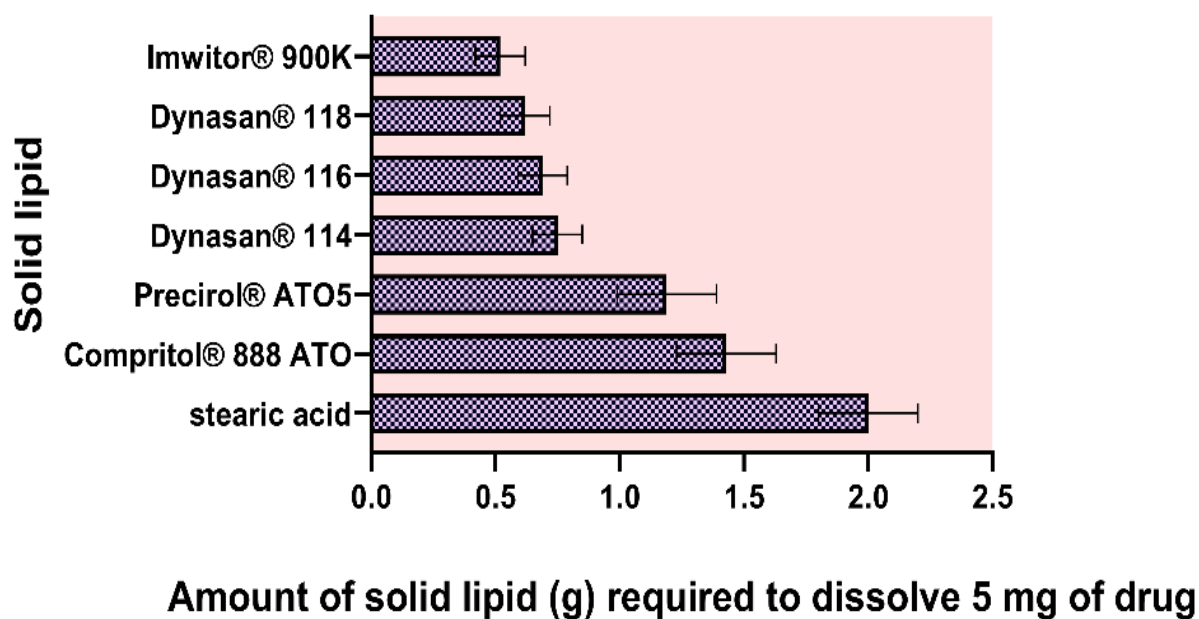


Figure 1. Screening of solid lipids for their ability to solubilize Paclitaxel

2.2. Preparation of solid lipid nanoparticle (SLN) of Paclitaxel

Solid lipid nanoparticles (SLNs) are colloidal structures formulated using solid lipids as a matrix, stabilized by emulsifiers in an external medium. This formulation enhances permeability through the fluidization of the membrane and solubilization of the lipids in the endothelial cell membrane, achieved through the emulsifier effect [25]. To select an appropriate emulsifier that can effectively stabilize the internal phase during emulsification, four different emulsifiers were screened: pluronic F68, polyvinyl alcohol (PVA), Tween 80, and sodium oleate. While keeping other process and formulation parameters constant, the results (not shown) indicated that sodium oleate provided the smallest particle size (below 200 nm) with an acceptable Polydispersity Index (PDI) of less than 0.1. Sodium oleate, being a lipophilic surfactant, possesses great potential to facilitate drug delivery through the lymphatic route [26]. Consequently, for further optimization of the formulation, sodium oleate was selected as the surfactant of choice. Its excellent stabilizing properties and ability to reduce the particle size are crucial factors contributing to its selection in the development of the optimized SLN formulation.

2.3. Experimental design

The emulsification/evaporation method was employed to formulate seventeen Paclitaxel (PTX) Solid Lipid Nanoparticle (SLN) formulations based on the selected experimental design. PTX content in the formulations was quantified using an HPLC method, which was developed and validated. The HPLC run time was set to 10 minutes, and PTX retention time was determined to be 6.9 minutes. The regression equation $A = 20.101 C + 0.775$, where A represents the area and C is the concentration of PTX, was obtained with a high correlation coefficient ($r^2 = 0.9999$). The limit of detection (LOD) was found to be $0.4 \mu\text{g/mL}$, and the limit of quantification (LOQ) was determined to be $0.9 \mu\text{g/mL}$. The precision of the method was evaluated with inter- and intra-precision, yielding values of 1.1-2.1% and 1.5-2.1%, respectively. Table 1 presents the observations of % entrapment efficiency (% EE) and particle size for all seventeen batches of PTX SLNs.

The selected independent factors were found to influence the two measured responses (particle size and % EE). The particle size ranged from 172 to 202 nm across all batches, with % EE values ranging from 57% to 88%. The response models for % EE (Y1) and particle size (Y2) were determined to be Linear and Quadratic, respectively. The Linear model showed a good fit for % EE (Y1), while the Quadratic model fit well for particle size (Y2) with higher R2 values, as shown in Table 2.

Table 1. The composition of various batches of Box-behnken design and their obtained values for dependent variables.

Run	Independent Variable			Dependent Variable	
	X1- Amount of Lipid	X2- % Surfactant concentration (% v/v)	X3- No. of Sonication cycles	Y1- Particle size	Y2- % Entrapment efficiency
1	10	15	15	183	79
2	5	12.5	15	176	67
3	5	15	10	172	69
4	10	12.5	10	188	77
5	10	10	15	186	70
6	15	10	10	202	80
7	10	10	5	193	70
8	10	12.5	10	188	77
9	10	12.5	10	188	77
10	5	10	10	185	57
11	10	12.5	10	188	77
12	15	12.5	15	192	83
13	5	12.5	5	182	67
14	10	12.5	10	188	77
15	15	12.5	5	198	82
16	10	15	5	190	79
17	15	15	10	193	88

Table 2. Model Summary statistics.

Model	R2	Adjusted R2	Predicted R2	SD	Remarks
Response (Y1)					
Linear	0.9475	0.9354	0.8904	1.84	Suggested
2FI	0.9523	0.9236	0.7560	2.00	
Quadratic	0.9559	0.8992	0.2944	2.30	
Cubic	1.0000	1.0000		0.0000	Aliased
Response (Y2)					
Linear	0.9440	0.9311	0.9031	1.96	Suggested
2FI	0.9488	0.9180	0.8211	2.14	
Quadratic	0.9824	0.9599	0.7190	1.50	Suggested
Cubic	1.0000	1.0000		0.0000	Aliased

The ANOVA (Analysis of Variance) feature of the software was utilized to determine the polynomial equations based on multiple statistical parameters. Table 3 displays the findings of the ANOVA study. The model F-values for % EE (Y1) and particle size (Y2) were 78.19 and 43.53, respectively, indicating that the selected linear and quadratic models were significant for both responses. Additionally, the "prob > F" value of 0.05 in Table 3 indicates the significance of the model terms. Overall, the experimental design, along with statistical analysis, allowed the identification of factors influencing the % EE and particle size of PTX SLNs, leading to the optimization of the formulation for enhanced drug delivery properties.

In the case of response Y1 (particle size), all three independent parameters were found to have a significant effect on the response. Values greater than 0.1000 indicated that the model terms were not significant. The adequate precision of 24.121 suggested that the signal-to-noise ratio was adequate, indicating a reliable model. With the third component held constant, these plots were used to examine how two independent factors interact with responses. Figures 2a,3a-c illustrate the graphs obtained for replies Y1 and Y2. Figures 2b,3d shows the perturbation plots.

Table 3. ANOVA for response surface quadratic model.

Source	Y1		Y2	
	F	P>F	F	P>F
Model	78.19	< 0.0001	43.52	< 0.0001
X1	180.72	< 0.0001	296.06	< 0.0001
X2	28.92	< 0.0001	80.22	< 0.0001
X3	24.93	0.8204	0.0556	0.8204
< 0.0001			1.78	0.2242
< 0.0001			0.1111	0.7486
< 0.0001			0.0000	1.0000
0.8204			4.94	0.0616
0.2242			6.58	0.0373
0.7486			0.7310	0.4209

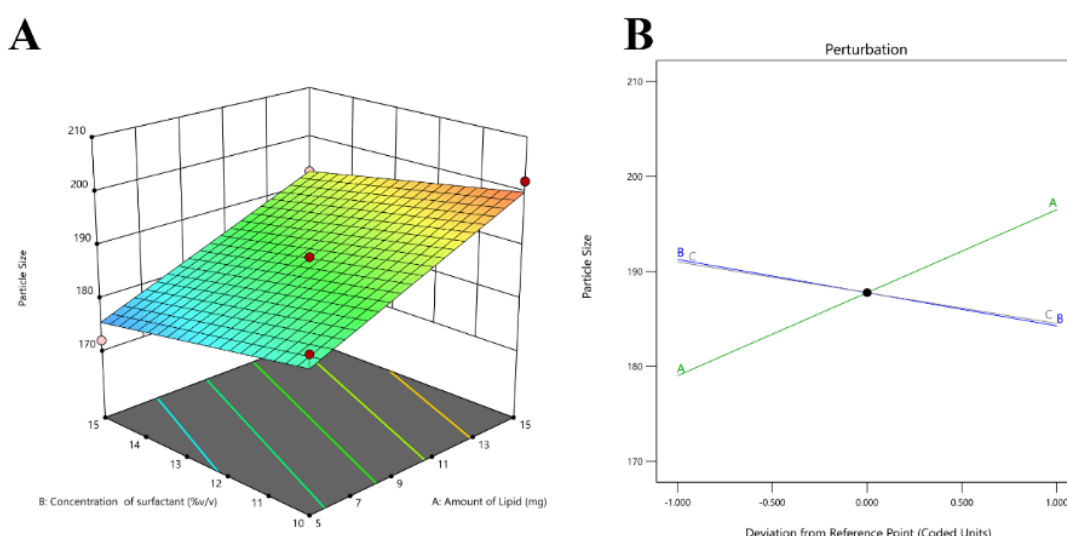


Figure 2. Response surface plot three-dimension showing effect of; (A) Amount of Lipid (X1) and Concentration of Surfactant (X2), (B) Perturbation plot showing effect of Amount of Lipid (X1), Concentration of Surfactant (X2) and No. of Sonication Cycle (X3) on particle size.

The following Linear equation can be used to calculate the influence of X1, X2 and X3 parameters on particle size.

$$Y1 = 187.76 + 8.75X1 - 3.5X2 - 3.25X3 \quad (3)$$

Positive coefficients before a factor (X1, X2, or X3) in the regression equation indicate that the particle size (Y1) increases as the corresponding factor increases. Conversely, negative coefficients indicate that the particle size decreases as the corresponding factor increases. Particle size increases in proportion to the amount of lipid (X1) consumed in the formulation. This effect might be attributed to the increase in dispersion viscosity caused by higher lipid content, resulting in higher surface tension and ultimately leading to larger particle sizes [23]. Particle size decreases as the number of sonication cycles (X2) increases. Increased sonication helps in achieving a more uniform size distribution and reduces particle agglomeration, resulting in smaller particle sizes. Particle size also decreases with an increase in surfactant concentration (X3). Higher surfactant levels can stabilize the nanoparticles more efficiently, preventing aggregation and leading to smaller particle sizes. The perturbation plot further justifies the impacts of these independent variables (X1, X2, and X3) on particle size (Y1) and provides additional insights into the relationship between the formulation parameters and the response. These findings are valuable in optimizing the formulation

process to achieve the desired particle size for PTX-loaded solid lipid nanoparticles with improved drug delivery properties.

Similarly, X1, X2 and X3 were discovered to be important determinants for response Y2, percent entrapment efficiency. were shown to be significant factors for response Y2, percent entrapment efficiency. The 24.12 "adequate precision" suggests a good signal. The derived quadratic equation is:

$$Y_2 = 77 + 9.125X_1 + 4.75X_2 + 0.125X_3 - 1X_1X_2 + 0.2500X_1X_3 + 0X_2X_3 - 1.625 X_{12} - 1.875X_{22} - 0.625X_{32}$$

The greater value before X1 suggests that the percent entrapment efficiency was significantly impacted by lipid and surfactant. The impacts of all three parameters on entrapment effectiveness were demonstrated using response surface plots. When the lipid amount increased in proportion to the drug, higher amount of PTX could be matrixed within lipid, increasing entrapment efficiency.

Design expert software was used for numerical optimization to produce an improved formulation. As response constraints, the various levels of desirability were fed into the software. The objective was to find the best formulation that maximizes drug entrapment while keeping the particle size within a specified range. The levels of independent factors predicted were 15 mg of lipid, 15 percent v/v surfactant concentration, and 12 number of sonication cycles. The preparation and analysis of this new batch of SLNs was done and result of responses were validated by calculating percent error. The model predicted the values as 187.75 nm particle size (Response Y1) and 77% entrapment efficiency (Response Y2). The observed values obtained were 191.14 nm (Y1) and 78.5 % (Y2) with error of 1.8 and 1.94 respectively. This demonstrated the efficacy of the optimization technique.

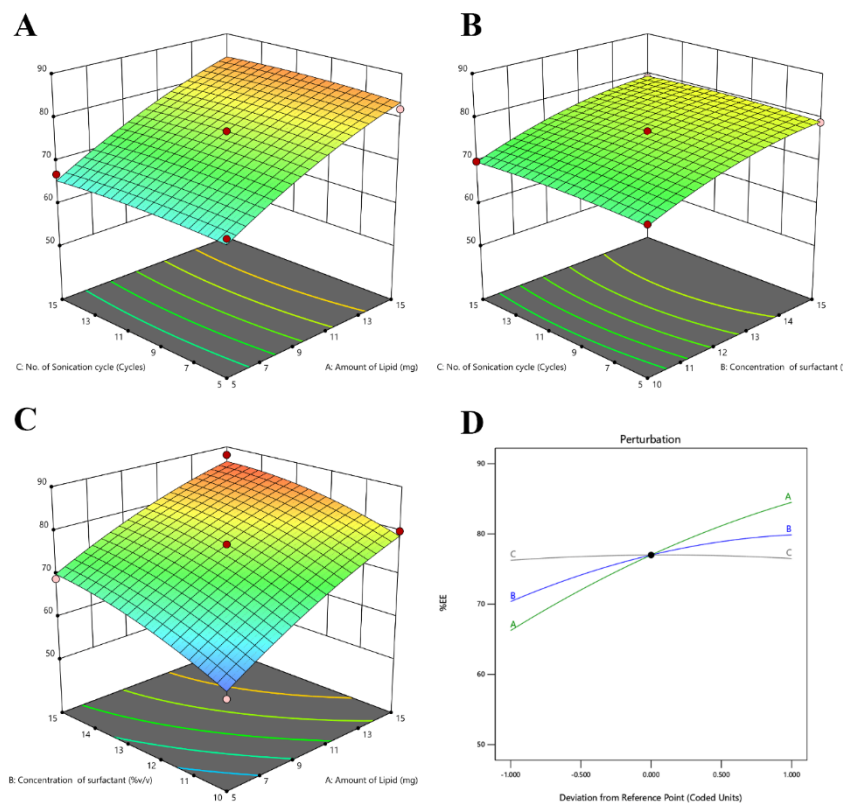


Figure 3. Response surface plot three-dimension showing effect of; (A) Amount of Lipid (X1) and No of Sonication Cycle (X3), (B) Concentration of Surfactant (X2) and No of Sonication cycle (X3), (C) Amount of Lipid (X1) and Concentration of Surfactant (X2), (D) Perturbation plot showing effect of Amount of Lipid (X1), Concentration of Surfactant (X2) and No. of Sonication Cycle (X3); on % Entrapment Efficiency.

2.4. Drug excipient compatibility study

2.4.1 Fourier transform- infrared spectroscopic (FT-IR) analysis

The purpose of the FT-IR investigation was to determine whether PTX was compatible with the formulation's excipients. The FT-IR spectrum of PTX (Figure 4A) showed characteristic peaks of N-H/O-H stretching vibration (3511-3300 cm^{-1}), CH_2 asymmetric and symmetric stretching vibrations (2917 and 2849 cm^{-1}), C-N stretching vibrations (1274 cm^{-1}), $\text{C}=\text{O}$ stretching vibration from ester group (1734 cm^{-1}) and C-O stretching at 1049 cm^{-1} . The peaks were similar to that reported in literature. The FT-IR spectrum of Imwitor K900 (Figure 4B) showed characteristic peaks of O-H stretching (3307 cm^{-1}), CH_2 stretching vibrations (2916 and 2955 cm^{-1}), C-N stretching vibrations (1273 cm^{-1}) and carbonate ion stretching (1419 cm^{-1}). The physical mixture spectrum (Figure 4C) and formulation (Figure 4D) showed presence of the characteristic peaks of PTX. This indicated that PTX was compatible with the excipients of formulation).

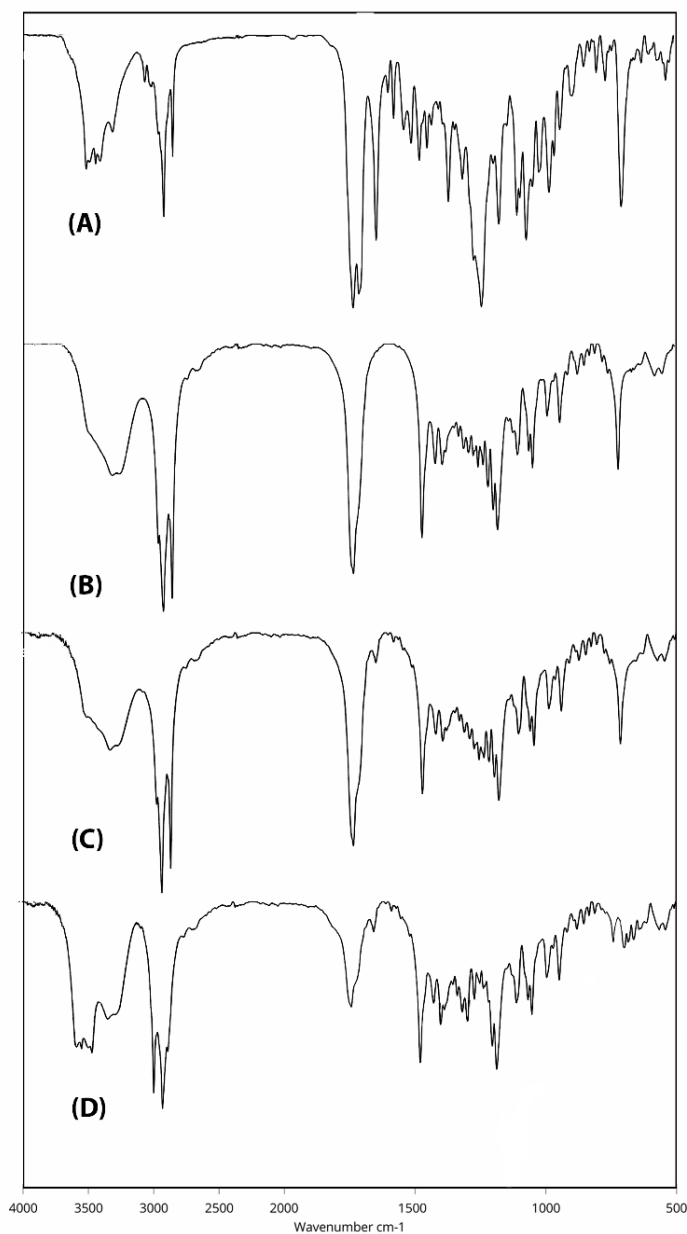


Figure 4. FTIR spectra of (A) PTX, (B) Imwitor 900K (C) Physical Mixture of PTX and Imwitor 900K (D) PTX loaded SLN.

2.4.2 Differential scanning calorimetry:

The DSC (Differential Scanning Calorimetry) study was conducted to investigate the physical form of PTX in a mixture and after loading it into SLNs. Figure 5 shows the DSC thermograms of PTX and Imwitor K900. PTX exhibited an endothermic peak at 225°C, indicating its melting point, while Imwitor K900 showed an endothermic peak at 65°C, indicating its own melting point [27]. In the case of the physical mixture of PTX and Imwitor K900 and the lyophilized SLNs, a peak was observed at 65°C, indicating the presence of Imwitor K900 in both samples. However, there was no endothermic peak observed at 225°C, suggesting the absence of PTX in its crystalline form. This indicates that PTX underwent conversion to an amorphous structure within the lipid matrix of the SLNs. Additionally, in the lyophilized formulation sample, there was an endothermic peak observed at 97°C. This peak can be attributed to the presence of trehalose, which indicates its melting at this temperature. The absence of the PTX endothermic peak and the presence of peaks related to Imwitor K900 and trehalose suggest successful entrapment of PTX in the lipid matrix of the SLNs, resulting in an amorphous drug structure. This is an essential finding as the amorphous state of the drug can enhance its solubility and bioavailability, thereby improving its therapeutic efficacy when delivered using the SLN system.

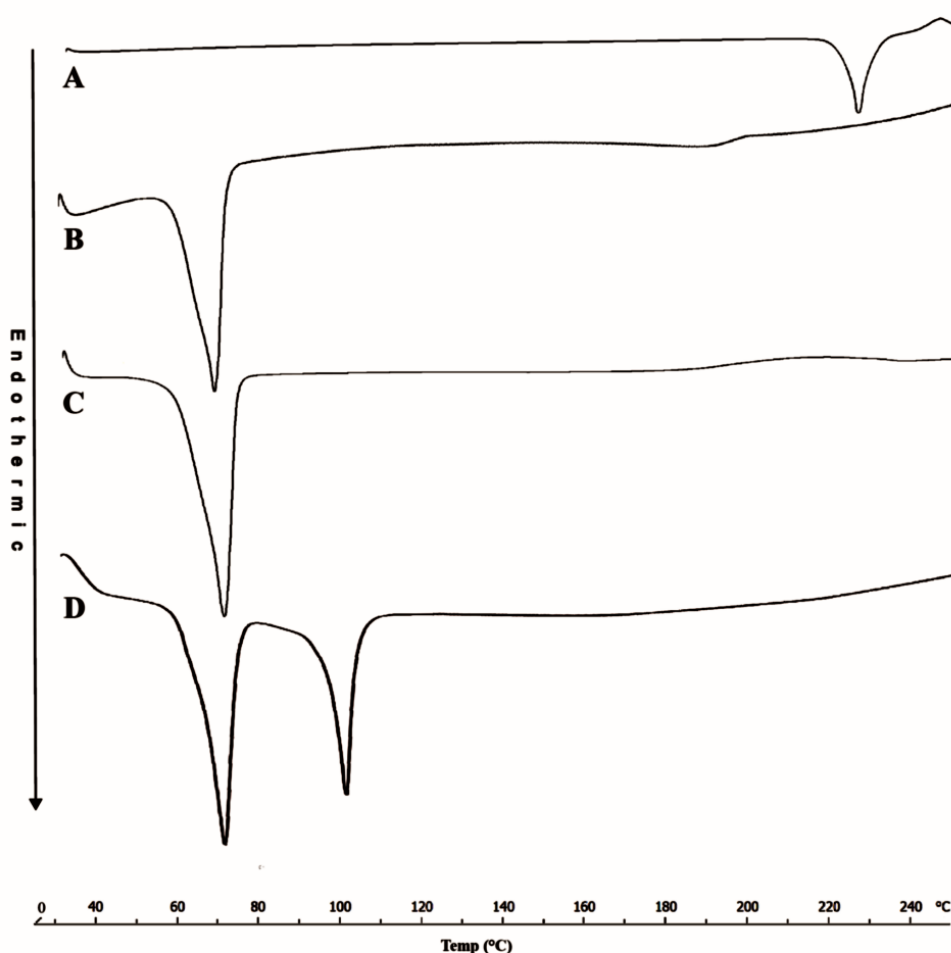


Figure 5. DSC graph of (A) PTX, (B) Imwitor 900K (C) Physical Mixture of PTX and Imwitor 900K (D) Lyophilized PTX loaded SLN.

2.5. Morphology study

Figure 6a and 6b shows TEM and SEM images of PTX-SLNs, respectively. Both the images showed non-aggregated particles and spherical shape. The diameter as obtained through TEM image was in accordance with the particle size analysis through Malvern Zeta Sizer.

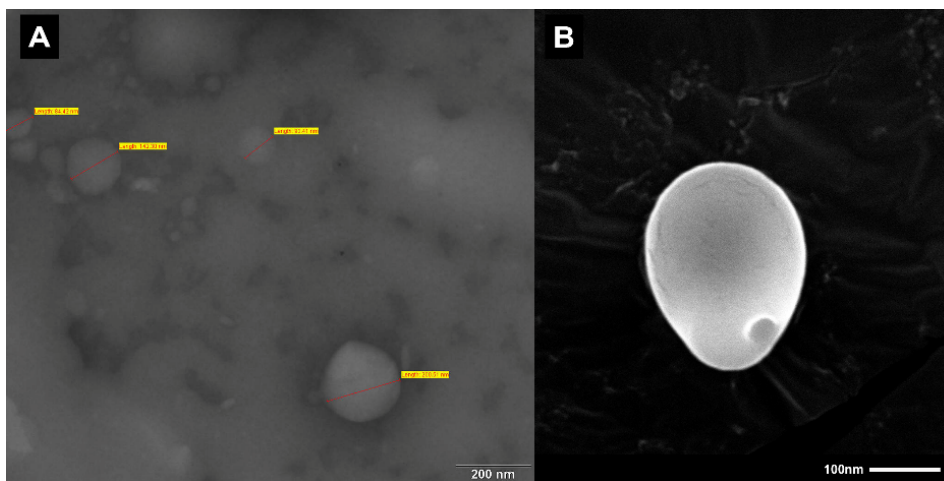


Figure 6. Image of (A) TEM of PTX loaded SLNs (B) SEM of lyophilized PTX loaded SLN.

2.6. *In-vitro* release of paclitaxel

The *in-vitro* release study provides valuable insights into the behavior of a drug through the gastrointestinal tract (GIT). In this study, SGF and SIF were used to mimic the dissolution environment in GIT. Figure 7 illustrates the cumulative release of PTX-SLNs and marketed formulation in SGF for 2 hr and SIF for 22 hr. It was observed that the marketed formulation released 96.1 % PTX, whereas only 65.3 % of PTX was released from PTX-SLNs within 48 hr. This indicates that the SLN formulation exhibited sustained release behavior compared to the marketed formulation. The sustained release can be attributed to the lipidic nature of the nanoparticles, which allows for controlled and prolonged drug release overtime. The sustained release of PTX from the SLN formulation is highly desirable as it enhances lymphatic absorption capacity of the nanoparticles given that nanoparticles. The intact nanoparticles in the GIT persist for an extended period, leading to prolonged drug exposure and increased chances of lymphatic absorption. Additionally, PTX is known to be a substrate of P-glycoprotein (P-gp), a transporter protein that can pump drugs out of cells, thus reducing their effectiveness. The enhanced lymphatic absorption facilitated by the SLNs can help to reduce P-gp efflux, leading to improved drug bioavailability and efficacy [6, 28].

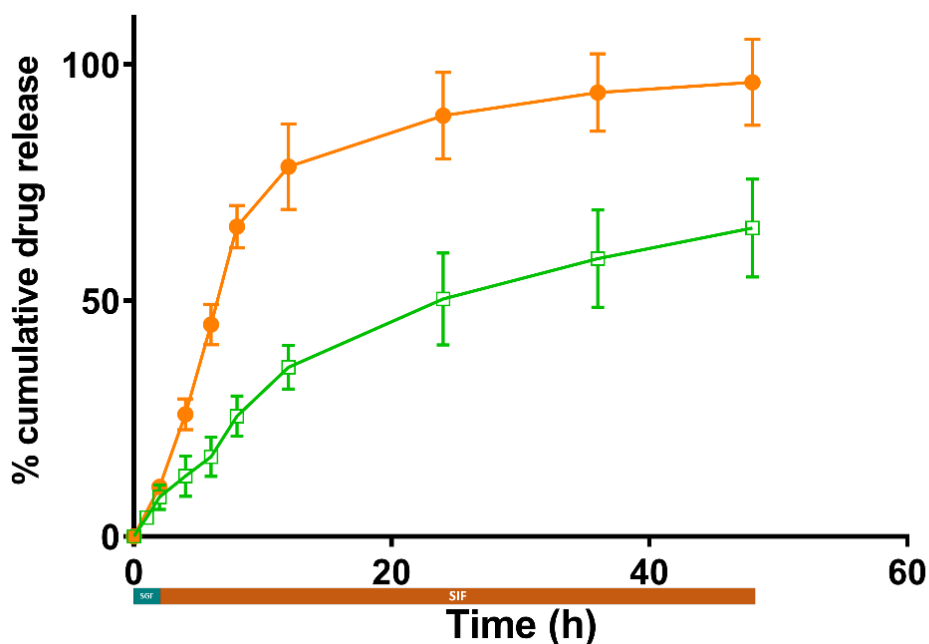


Figure 7. *In-vitro* PTX release from PTX-SLNs (-□-) and marketed preparation (-●-) in simulated gastric fluid and simulated intestinal fluid.

2.7. In-vivo study

The quantification of PTX in plasma samples were performed using the developed RP-HPLC method. PTX was detected at 7.2 min in a total run time of 10 min. The regression equation obtained was $A = 16.646 C + 1.776$ with r^2 value of 0.9997, indicating the accuracy of the method. The limit of detection and quantification were observed as 0.4 and 0.8 $\mu\text{g/mL}$, respectively, confirming the suitability of the detection. Figure 8 displays the plasma concentration-time curve of PTX in rats. The C_{max} of the drug in the formulation ($C_{\text{max}} = 300 \text{ ng/mL}$) was increased by 3.75 fold compared to the marketed formulation ($C_{\text{max}} = 80 \text{ ng/mL}$). This increase in C_{max} can be attributed to the improved solubility of the drug in the gastric media due to reduced particle size and presence of lipid in the formulation, which enhances solubilization of the drug and leads to a higher concentration gradient across GIT tract, thereby improving absorption. Additionally, the controlled release of PTX from PTX-SLNs resulted in a delayed t_{max} (2 hr) compared to the marketed product ($t_{\text{max}} = 1.5 \text{ hr}$). This delayed t_{max} is due to the controlled release of the drug from the formulation and the nanoparticles remaining intact for a longer period of time in GI media than the marketed product. Moreover, AUC_{0-t} and $AUC_{0-\infty}$ was found to be 1178 ± 103.3 and $311 \pm 43.2 \text{ ng/mL}$ (for PTX-SLNs) while 1216 ± 112.4 and $401 \pm 3.1 \text{ ng/mL}$ for marketed preparation. The bioavailability of PTX from PTX-SLN formulation was found to be enhanced by 2.4 fold compared to marketed product. This increased bioavailability further supports the enhanced absorption of PTX from the SLN formulation, contributing to its improved therapeutic efficacy and potential for cancer therapy.

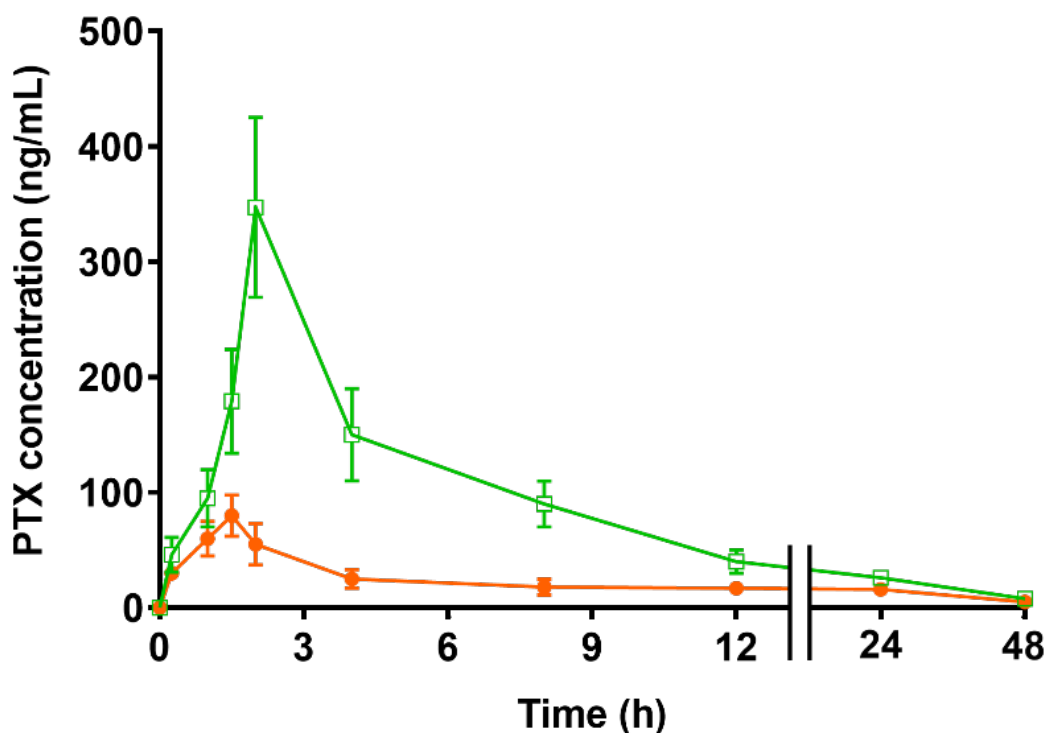


Figure 8. The plasma concentration of PTX-time curve in rats after oral administration of PTX loaded SLNs (-□-) and marketed formulation (-●-).

2.8. Stability study

The optimized formulation was stable over 6 months period (Table 4). The entrapment efficiency was found to decrease insignificantly in 6 months period that might be because of drug expulsion during its storage. The particle size and assay remained nonsignificant during the time period indicating the stability of prepared formulation.

Table 4. Results of stability study of PTX loaded SLNs

Day	Particle Size	% assay	Entrapment efficiency
0	191.1 ± 0.45	78.5 ± 0.34	99.80 ± 0.21
30	197.2 ± 0.36	76.3 ± 0.45	99.45 ± 0.22
60	196.2 ± 0.36	74.2 ± 0.35	99.52 ± 0.23
90	198.5 ± 0.35	72.3 ± 0.25	99.27 ± 0.26
120	201.4 ± 0.36	70.3 ± 0.36	99.39 ± 0.25
150	200.5 ± 0.44	70.2 ± 0.35	99.30 ± 0.22
180	205.2 ± 0.32	68.6 ± 0.45	99.32 ± 0.23

The values (n=3) are represented as mean ± SD

3. CONCLUSION

In conclusion, the incorporation of PTX into a lipid carrier, specifically solid lipid nanoparticles (SLNs), has proven to be a promising approach to enhance the drug's efficiency by increasing its solubility and bioavailability. The PTX was successfully loaded into the SLNs, and in-vitro studies demonstrated a controlled drug release profile, which could be beneficial for the intact delivery of nanoparticles to the lymphatic system. The optimized PTX-SLN formulation exhibited a delayed time to reach maximum concentration (t_{max}) compared to the marketed Taxol[®] formulation. However, the enhanced bioavailability observed with the PTX-SLN formulation, which was 2.4-fold higher than that of Taxol[®], indicates the potential superiority of this lipid-based approach for drug delivery in cancer therapy. The findings of this study highlight the advantages of using lipid-based carriers like SLNs to overcome the challenges associated with PTX's low solubility and permeability. The controlled drug release and improved bioavailability of PTX-SLNs offer promising prospects for more effective and targeted cancer treatment. This research contributes valuable insights into the development of lipidic drug delivery systems, which could pave the way for the successful translation of PTX-SLNs into clinical applications, ultimately benefiting cancer patients with improved therapeutic outcomes.

4. MATERIALS AND METHODS

4.1 Materials

Dynasan114, Dynasan 116, Dynasan 118 and Imwitor 900K were gifted by IOI Oleo GmbH Germany. Paclitaxel was offered as a free sample by Cadila Healthcare Ltd. Precirol ATO-5 and Compritol 888 were gifted by Gattefosse (Germany). Tween 80 was procured from loba chemical Pvt Ltd. Methanol was purchased from Loba Chemical Pvt. Ltd. Sodium oleate, Pluronic F68 and polyvinyl alcohol were purchased from Hi-Media Pvt Ltd.

4.2 Selection of lipid

Briefly, 5 mg PTX was placed in a glass vial and various solid lipids (Stearic acid, Compritol 888, Precirol ATO-5, Dynasan 114, dynasan116, dynasan118 and Imwitor 900K) were added until the drug completely dissolved, resulting in a clear solution. The vial was then maintained at a temperature 10°C higher than the respective melting point of the lipid. To check for the presence of drug crystals, samples were observed under a microscope. The amount of solid lipid required to melt PTX was measured, and each measurement was conducted three times [29,30].

4.3 Preparation of solid lipid nanoparticle (SLN)

To produce PTX-loaded solid lipid nanoparticles, the solvent emulsification/evaporation method was employed [31]. Initially, Imwitor 900K and PTX were dissolved in dichloromethane (DCM) to form the non-aqueous phase. In a separate container, an aqueous phase was created using sodium oleate dissolved in 10 mL of distilled water. The non-aqueous phase was then added dropwise into the aqueous phase, which was continuously stirred on a magnetic stirrer, and the organic solvent was allowed to evaporate at room temperature. After the evaporation, the resulting SLN dispersion was sonicated for 5 min with 3 sec pulses at 45% amplitude using a VCX-500, Vibra cell, USA. Subsequently, the nanoparticles were further sonicated at 10,000 rpm for 10 min using a Microcentrifuge (Spinwin MC-01) to settle any untrapped drug molecules. The supernatant containing the nanoparticles, was collected. To optimize the formulation and

process parameters, an experimental design was utilized. Following the optimization, the optimized batch was lyophilized using Trehalose at a concentration of 20 mg/mL in the Vertis Lyophilizer (Vertis Advantage-plus, USA).

4.4 Experimental design

To achieve nanometric-sized particle preparation, various parameters play a crucial role, with key factors including the drug-lipid ratio, stabilizer concentration, sonication cycle and drug loading. To optimize the formulation, we employed an experimental design approach using the Box-Behnken design (Design Expert, Version 8.0.3, StatEase Inc., MN) [32]. This design allowed us to study the effects of three independent parameters: the amount of lipid (X_1), surfactant concentration (X_2) and number of sonication cycles (X_3) on two dependent parameters: particles size (Y_1) and % encapsulation efficiency (EE) (Y_2). For this study, we considered low, medium, and high levels of lipid, which were coded as 5, 10 and 15 mg, respectively. The sodium oleate concentration was set at 5, 7.5 and 10 %v/v, representing low, medium, and high levels. Additionally, the number of homogenization cycles was set at 10, 15, 20. Throughout the optimization process, we applied constraints to ensure that the particle size remained within a specified range and maximized the encapsulation efficiency (EE). This approach allowed us to identify the optimal formulation with nanometric-sized particles and high encapsulation efficiency.

4.5 Determination of particle size

Utilizing the Malvern Zetasizer ZS 90 (Malvern Instrument, Worcestershire, UK), several trial batches of PTX-SLNs was examined for particle size [33]. Distilled water was used to dilute the samples, filled in disposable sizing cuvette and analyzed in triplicate. After lyophilization, PTX-SLNs was assessed for the particle size.

4.6 Estimation of drug loading and entrapment efficiency

The HPLC analysis was performed using Shimadzu LC20AT system from Japan, with a C18 Octa decyl silane (dimensions- 250 mm x 4.6 mm x 5 μ m, Thermo Fischer Scientific, USA). The mobile phase, consisting of acetonitrile, methanol, and water in ratio of 40: 35: 25 was adjusted to a pH of 3 using glacial acetic acid (1% v/v). For the calibration curve, PTX concentrations ranging from 1 to 50 μ g/mL were prepared in methanol and injected in 20 μ L, with a runtime of 10 min at a flowrate of 1mL/min. The samples were analyzed using UV-Visible detector (227 nm wavelength). The method was validated as per ICH guidelines (data not shown).

The entrapment efficiency of various batches from the experimental design was determined by removing free drug through centrifugation and analyzing the entrapped drug present in the supernatant. Centrifugation was performed at 4°C using a REMI Centrifuge (REMI Instruments, Mumbai, India) at a speed of 10,000 rpm for 10 min. Free drug in dissolved form in supernatant was removed using gel exclusion chromatography [34]. The nanoparticle-containing supernatant was dissolved in a solvent mixture of chloroform: methanol in ratio of 3:7, followed by analysis using the RP-HPLC method [35]. For the lyophilized formulation, reconstitution was done before centrifugation, and the entrapment efficiency (EE) was calculated as per following [33].

$$\% EE = \frac{\text{actual amount of PTX in nanoparticles}}{\text{total amount of PTX added}} * 100 \quad (1)$$

For drug loading,

$$\% \text{ drug loading} = \frac{\text{actual amount of PTX in nanoparticles}}{\text{total amount of nanoparticles}} * 100 \quad (2)$$

4.7 Drug excipient compatibility study

4.7.1 Fourier transform- infrared spectroscopic (FT-IR) analysis

FT-IR analysis was conducted on PTX, Imwitor 900K, the physical mixture of PTX and Imwitor 900K and the optimized PTX-SLNs to assess any potential interactions between the drug and excipients. The samples were finely pulverised and mixed with potassium bromide before being examined using an FT-IR spectrophotometer (Nicolet 6700 FT-IR spectrometer, Thermo Fischer scientific, United states) [36].

4.7.2 Differential scanning calorimetry (DSC)

Thermodynamic changes in PTX, the physical mixture (PTX: lipid ratio of 1:1), and lyophilized SLNs were analyzed using Differential Scanning Calorimetry (DSC). The samples were placed in standard aluminum DSC pans and heated a rate of 2°C/min under a nitrogen atmosphere in the DSC-60 instrument

(Schimadzu, India). The temperature range covered during the analysis was 20-250°C, and the flow rate of nitrogen was maintained at a constant value of 40 mL/min [37].

4.8 Morphology Study

Microscopic examination of the optimized PTX-SLNs was conducted using Transmission electron microscopy (TEM). The sample was placed on a 3 mm copper grid coated with carbon and dried under atmospheric condition. Subsequently, the sample was stained with phosphotungstic acid for 30 sec. Observations were made using a transmission electron microscope (Hitachi H-7500, Japan) equipped with a 200 kV accelerating voltage after the staining process [38]. For the examination of the outer surface of nanoparticles following lyophilization, scanning electron microscopy (SEM) was utilized. The sample was coated with platinum for 300 seconds using an ion sputter. Images were captured at a 15 kV acceleration voltage using a backscattered electron detector in a scanning electron microscope (JSM- 6360, Jeol, USA). The observation was performed at $25 \pm 2^\circ\text{C}$ [39].

4.9 *In-vitro* release of PTX

To assess the release pattern of PTX-SLN and the marketed formulation under an *in-vitro* conditions, the dialysis bag method was utilized [40]. In this method, a 5 mg of PTX sample was placed in a dialysis tube with a molecular weight cut-off (MWCO) of 12000 Da (Hi-Media, India). The dialysis bag was then immersed in a beaker containing 40 mL of simulated gastric fluid (SGF) with a pH of 1.2 at temperature of $37^\circ\text{C} \pm 2^\circ\text{C}$ and stirred for 2 hr. After the initial 2 hr period, the dissolution media was removed and 40 mL of simulated intestinal fluid (SIF) with a pH of 6.8 was added. The study was continued for an additional 24 hr. At regular intervals, 1mL samples were taken, and the media was replenished with the same volume of fresh media. The removed samples were then lyophilized, reconstituted in 1 mL of methanol, and amount of PTX was estimated using HPLC [41]. The percentage drug release was calculated based on the amount of PTX released from the dialysis bag overtime. This method allowed for the evaluation of the *in-vitro* release behavior of PTX from the SLNs and the marketed formulation.

4.10 *In-vivo* study

Female Sprague Dawley rats weighing 200 ± 20 g were used in the pharmacokinetic study. The experiment was reviewed and approved by Institutional Animal Ethics Committee (Protocol No: RPCP/IAEC/2022-23/R13). The rats were divided into three groups, each consisting of six animals. Before the experiment, the rats were fasted overnight. The first group was administered PTX-SLNs, the second group received Taxol® and the third group served as the negative control and received saline. The dose of PTX administered orally to the first two groups was 10mg/kg. The samples were administered using infant feeding tube and syringe. Blood samples were collected at different time points: 0.25, 0.5, 1, 2, 4, 8, 12, 24, and 48 hours after drug administration through the retro-orbital venous plexus punctures. Each blood sample was centrifuged for 10 minutes at 4000 rpm to separate plasma which was then stored at -20°C until RP-HPLC evaluation. The obtained data were analyzed using non-compartmental model pharmacokinetics with the help of Kinetica software (Version 5.1) to determine various pharmacokinetic parameters. These analyses allowed for the characterization of the drug's behavior in the rats after administration of PTX-SLNs, Taxol®, and saline.

To quantify PTX in plasma samples, an RP-HPLC method was employed with the same chromatographic conditions as used for the estimation of the drug. However, the drug extraction was performed using the protein precipitation technique. For calibration, PTX was first dissolved in methanol and then diluted with plasma to achieve concentrations ranging from 4 to 40 $\mu\text{g}/\text{mL}$. Each solution (100 μL) was spiked with 300 μL of methanol and centrifuged at 4000 rpm, 4°C , for 10 minutes to collect the supernatant containing the drug in methanol. The plasma was retained in precipitated form during this step. The final concentration of the drug in the plasma ranged from 1 to 10 $\mu\text{g}/\text{mL}$. The analysis was performed in triplicate to ensure the accuracy and reliability of the results. The RP-HPLC method allowed for the precise quantification of PTX in the plasma samples, enabling pharmacokinetic analysis and assessment of drug concentration over time.

4.11 Stability studies

The stability of the optimized formulation was evaluated following the guidelines provided by the International Council for Harmonisation (ICH) in Q1A (R2), 2003. The formulation was placed in a vial, sealed, and then stored in a stability chamber at controlled conditions of $25 \pm 2^\circ\text{C}$ and $60 \pm 5\%$ relative humidity (RH). At regular intervals of 15 days, starting from day 0, samples were collected from the vial and assessed for several parameters. These parameters included particle size, % assay (to determine the amount of active drug present), and entrapment efficiency (to measure the amount of drug retained in the nanoparticles). The evaluation at each time point allowed for the monitoring of the formulation's stability over an extended period. By analyzing these stability data, researchers could gain insights into the long-term performance and potential degradation or changes in the optimized formulation under the specified storage conditions. This assessment is crucial for ensuring the quality and shelf-life of the formulation before potential clinical or commercial applications.

4.12 Statistical Analysis

Throughout the entire study, all measurements were conducted three times, and the data are presented as the mean \pm standard deviation. The GraphPad Prism software (Version 6, USA) was utilized for data analysis. Statistical significance was determined using the p-value, and a value less than 0.05 was considered as significant. By conducting measurements multiple times and reporting the mean and standard deviation, the researchers aimed to provide a more reliable and representative representation of the results. The use of statistical analysis and determination of significance helps in drawing valid conclusions from the data and ensures the robustness of the findings.

Acknowledgements: The work was funded by Charotar University of Science and Technology under CHARUSAT Research Grant (Reference No: CHA/RC/RG/2019/02/147). The authors acknowledge Sophisticated Instrument centre for Applied research and testing (SICART), Vallabh Vidyanagar, Gujarat, India for providing TEM facility.

Author contributions: Concept - J.D., A.M.; Design - J.D., S.P., A.P.; Supervision - J.D.; Resources - A.M., T.P., A.P.; Materials - T.P., A.P.; Data Collection and/or Processing - T.P., A.P.; Analysis and/or Interpretation - J.D., T.P., A.P.; Literature Search - T.P., S.P.; Writing - J.D., S.P.; Critical Reviews - J.D., A.M., A.P., S.P.

Conflict of interest statement: The authors declared no conflict of interest.

REFERENCES

- [1] Homayun B, Lin X, Choi HJ. Challenges and recent progress in oral drug delivery systems for biopharmaceuticals. *Pharmaceutics*. 2019;11:1-29. <http://doi.org/10.3390/pharmaceutics11030129>.
- [2] Schenk M, Mueller C. The mucosal immune system at the gastrointestinal barrier. *Best Prac Res Clin Gastroenterol*. 2008;22:391-409. <http://doi.org/10.1016/j.bpg.2007.11.002>.
- [3] Kalepu S, Manthina M, Padavala V. Oral lipid-based drug delivery systems—an overview. *Acta Pharm Sinica B*. 2013;3:367-372. <http://doi.org/10.1016/j.apsb.2013.10.001>.
- [4] Fasinu P, Pillay V, Ndesendo VM, du Toit LC, Choonara YE. Diverse approaches for the enhancement of oral drug bioavailability. *Biopharm Drug Dispos*. 2011;32:185-209. <http://doi.org/10.1002/bdd.750>.
- [5] Patil OB, Manjappa AS, Kumbhar PS, Bhosale SP, Disouza JI, Salawi A, Sambamurthy U. Development of stable self-nanoemulsifying composition and its nanoemulsions for improved oral delivery of non-oncology drugs against hepatic cancer. *OpenNano*. 2022;7:100044. <http://doi.org/10.1016/j.onano.2022.100044>.
- [6] Aji Alex MR, Chacko AJ, Jose S, Souto EB. Lopinavir loaded solid lipid nanoparticles (SLN) for intestinal lymphatic targeting. *Eur J Pharm Sci*. 2011;42:11-18. <http://doi.org/10.1016/j.ejps.2010.10.002>.
- [7] Muchow M, Maincent P, Muller RH. Lipid nanoparticles with a solid matrix (SLN, NLC, LDC) for oral drug delivery. *Drug Dev Ind Pharm*. 2008;34:1394-1405. <http://doi.org/10.1080/03639040802130061>.
- [8] Ma P, Mumper RJ. Paclitaxel nano-delivery systems: A comprehensive review. *J Nanomed Nanotechnol*. 2013;4:1000164. <http://doi.org/10.4172/2157-7439.1000164>.
- [9] Varma MV, Panchagnula R. Enhanced oral paclitaxel absorption with vitamin E-TPGS: effect on solubility and permeability in vitro, in situ and in vivo. *Eur J Pharm Sci*. 2005;25:445-453. <http://doi.org/10.1016/j.ejps.2005.04.003>.
- [10] Kasim NA, Whitehouse M, Ramachandran C, Bermejo M, Lennernas H, Hussain AS, Junginger HE, Stavchansky SA, Midha KK, Shah VP, Amidon GL. Molecular properties of WHO essential drugs and provisional biopharmaceutical classification. *Mol Pharm*. 2004;1:85-96. <http://doi.org/10.1021/mp034006h>.

- [11] Wang H, Cheng G, Du Y, Ye L, Chen W, Zhang L, Wang T, Tian J, Fu F. Hypersensitivity reaction studies of a polyethoxylated castor oil-free, liposome-based alternative paclitaxel formulation. *Mol Med Rep.* 2013;7:947-952. <http://doi.org/10.3892/mmr.2013.1264>.
- [12] Zhao M, Lei C, Yang Y, Bu X, Ma H, Gong H, Liu J, Fang X, Hu Z, Fang Qiaojun F. Abraxane, the nanoparticle formulation of paclitaxel can induce drug resistance by up-regulation of P-gp. *PLoS one.* 2015;10:e0131429. <http://doi.org/10.1371/journal.pone.0131429>.
- [13] Pouton CW. Formulation of poorly water-soluble drugs for oral administration: physicochemical and physiological issues and the lipid formulation classification system. *Eur J Pharm Sci.* 2006;29:278-287. <http://doi.org/10.1016/j.ejps.2006.04.016>.
- [14] des Rieux A, Fievez V, Garinot M, Schneider YJ, Preat V. Nanoparticles as potential oral delivery systems of proteins and vaccines: a mechanistic approach. *J Control Rel.* 2006;116:1-27. <http://doi.org/10.1016/j.jconrel.2006.08.013>.
- [15] Brayden DJ, Jepson MA, Baird AW. Keynote review: intestinal Peyer's patch M cells and oral vaccine targeting. *Drug Discov Today.* 2005;10:1145-1157. [http://doi.org/10.1016/S1359-6446\(05\)03536-1](http://doi.org/10.1016/S1359-6446(05)03536-1).
- [16] Desai J, Khatri N, Chauhan S, Seth A. Design, development and optimization of self-microemulsifying drug delivery system of an anti-obesity drug. *J Pharm Bioallied Sci.* 2012;4:S21-22. <http://doi.org/10.4103/0975-7406.94124>.
- [17] Maharjan S, Singh B, Jiang T, Yoon SY, Li HS, Kim G, Gu MJ, Kim SJ, Park O, Han SH, Kang S, Yun C, Choi Y, Cho C. Systemic administration of RANKL overcomes the bottleneck of oral vaccine delivery through microfold cells in ileum. *Biomaterials.* 2016;84:286-300. <http://doi.org/10.1016/j.biomaterials.2016.01.043>.
- [18] Prabhu S, Ortega M, Ma C. Novel lipid-based formulations enhancing the in vitro dissolution and permeability characteristics of a poorly water-soluble model drug, piroxicam. *Int J Pharm.* 2005;301:209-216. <http://doi.org/10.1016/j.ijpharm.2005.05.032>.
- [19] Wissing SA, Muller RH. The influence of solid lipid nanoparticles on skin hydration and viscoelasticity--in vivo study. *Eur J Pharm Biopharm.* 2003;56:67-72. [http://doi.org/10.1016/s0939-6411\(03\)00040-7](http://doi.org/10.1016/s0939-6411(03)00040-7).
- [20] Sanchez-Lopez E, Espina M, Doktorovova S, Souto EB, Garcia ML. Lipid nanoparticles (SLN, NLC): Overcoming the anatomical and physiological barriers of the eye - Part II - Ocular drug-loaded lipid nanoparticles. *Eur J Pharm Biopharm.* 2017;110:58-69. <http://doi.org/10.1016/j.ejpb.2016.10.013>.
- [21] Uner M, Yener G. Importance of solid lipid nanoparticles (SLN) in various administration routes and future perspectives. *Int J Nanomedicine.* 2007;2:289-300.
- [22] Sawant KK, Dodiya SS. Recent advances and patents on solid lipid nanoparticles. *Recent Pat Drug Deliv Formul.* 2008;2:120-35. <http://doi.org/10.2174/187221108784534081>.
- [23] Mehnert W, Mader K. Solid lipid nanoparticles: production, characterization and applications. *Adv Drug Deliv Rev.* 2001;47:165-196. [http://doi.org/10.1016/s0169-409x\(01\)00105-3](http://doi.org/10.1016/s0169-409x(01)00105-3).
- [24] Peltier S, Oger JM, Lagarce F, Couet W, Benoit JP. Enhanced oral paclitaxel bioavailability after administration of paclitaxel-loaded lipid nanocapsules. *Pharm Res.* 2006;23:1243-1250. <http://doi.org/10.1007/s11095-006-0022-2>.
- [25] Kaur IP, Bhandari R, Bhandari S, Kakkar V. Potential of solid lipid nanoparticles in brain targeting. *J Control Rel.* 2008;127:97-109. <http://doi.org/10.1016/j.jconrel.2007.12.018>
- [26] Desai J, Thakkar H. Darunavir-Loaded Lipid Nanoparticles for Targeting to HIV Reservoirs. *AAPS PharmSciTech.* 2018;19:648-660. <http://doi.org/10.1208/s12249-017-0876-0>.
- [27] Zhang C, Qineng P, Zhang H. Self Assembly and characterization of paclitaxel-loaded N-octyl-O-sulfate chitosan micellar system. *Colloids Surf B Biointerfaces.* 2004;39:69-75. <http://doi.org/10.1016/j.colsurf.2004.09.002>.
- [28] Desai J, Patel T. Lymphatic targeting system using nano-formulation: Challenges and approaches. *Int J Pharm Sci Res.* 2021;12:2036-2048. [http://doi.org/10.13040/IJPSR.0975-8232.12\(4\).2036-48](http://doi.org/10.13040/IJPSR.0975-8232.12(4).2036-48).
- [29] Bhalekar M, Upadhaya P, Madgulkar A. Formulation and characterization of solid lipid nanoparticles for an anti-retroviral drug darunavir. *Appl Nanosci.* 2017;7:47-57. <http://doi.org/10.1007/s13204-017-0547-1>.
- [30] Harshita, Barkat MA, Rizwanullah M, Beg S, Pottoo FH, Siddiqui S, Ahmad FJ. Paclitaxel-loaded nanolipidic carriers with improved oral bioavailability and anticancer activity against human liver carcinoma. *AAPS PharmSciTech.* 2019;20:87. <http://doi.org/10.1208/s12249-019-1304-4>.
- [31] Sharma G, Rath G, Goyal A. Improved biological activity and stability of enzyme L-asparaginase in solid lipid nanoparticles formulation. *J Drug Deliv Ther.* 2019;9:325-329. <http://doi.org/10.22270/jddt.v9i2-s.2708>.
- [32] Gidwani B, Vyas A. Preparation, characterization, and optimization of altretamine-loaded solid lipid nanoparticles using Box-Behnken design and response surface methodology. *Artif Cells Nanomed Biotechnol.* 2016;44:571-580. <http://doi.org/10.3109/21691401.2014.971462>.
- [33] Pooja D, Tunki L, Kulhari H, Reddy BB, Sistla R. Optimization of solid lipid nanoparticles prepared by a single emulsification-solvent evaporation method. *Data in Brief.* 2016;6:15-19. <http://doi.org/10.1016/j.dib.2015.11.038>.
- [34] Bhatt P, Lalani R, Vhora I, Patil S, Amrutiya J, Misra A, Mashru R. Liposomes encapsulating native and cyclodextrin enclosed paclitaxel: Enhanced loading efficiency and its pharmacokinetic evaluation. *Int J Pharm.* 2018;536:95-107. <http://doi.org/10.1016/j.ijpharm.2017.11.048>.
- [35] Qiu N, Cai L, Wang W, Wang G, Cheng X, Xu Q, Wen J, Liu J, Wei Y, Chen L. Barbigeron-in-hydroxypropyl- β -cyclodextrin-liposomal nanoparticle: preparation, characterization and anti-cancer activities. *J Incl Phenom Macrocycl Chem.* 2015;82:505-514. <http://doi.org/10.1001/s10847-015-0533-8>.
- [36] Martins KF, Messias AD, Leite FL, Duek EA. Preparation and characterization of paclitaxel-loaded PLDLA microspheres. *Mat Res.* 2014;17:650-656. <http://doi.org/10.1590/S1516-14392014005000028>.

- [37] Dinda A, Biswal I, Chowdhury P, Mohapatra R. Formulation development and evaluation of paclitaxel loaded solid lipid nanoparticles using glyceryl monostearate. *J Appl Pharm Sci.* 2013;3:133. <http://doi.org/10.7324/APS.2013.3823>.
- [38] Shenoy VS, Rajyaguru TH, Gude RP, Murthy RS. Studies on paclitaxel-loaded glyceryl monostearate nanoparticles. *J Microencapsul.* 2009;26:471-478. <http://doi.org/10.1080/02652040802379902>.
- [39] Saboktakin MR, Tabatabaee RM, Maharramov A, Ramazanov MA. Design and characterization of chitosan nanoparticles as delivery systems for paclitaxel. *Carbohydr Polym.* 2010;82:466-471. <http://doi.org/10.1016/j.carbpol.2010.05.005>.
- [40] Desai J, Thakkar H. Mechanistic evaluation of lymphatic targeting efficiency of Atazanavir sulfate loaded lipid nanocarriers: In-vitro and *in-vivo* studies. *J Drug Deliv Sci Technol.* 2022;68:103090. <http://doi.org/10.1016/j.jddst.2021.103090>.
- [41] Chen Te, Tu L, Wang G, Qi N, Wu W, Zhang W, Feng J. Multi-functional chitosan polymeric micelles as oral paclitaxel delivery systems for enhanced bioavailability and anti-tumor efficacy. *Int J Pharm.* 2020;578:119105. <http://doi.org/10.1016/j.ijpharm.2020.119105>.